

AN APPROXIMATE QUEUING MODEL FOR PERFORMANCE EVALUATION OF APPLICATIONS RUNNING OVER THE WIRELESS CHANNELS

Dmitri Moltchanov, Yevgeni Koucheryavy, Jarmo Harju
Institute of Communication Engineering,
Tampere University of Technology,
P.O.Box 553, Tampere, Finland
e-mail: {moltchan,yk,harju}@cs.tut.fi

ABSTRACT

In this paper, we address the problem of performance evaluation of applications running over the wireless channels. Firstly, we develop an extension for existing wireless channel modeling techniques to the case of mobility-dependent behavior. Based on the amount of available information regarding a propagation environment we provide three parametrization methods. Then, to avoid computationally expensive physical layer simulations when performing performance evaluation studies we extend the proposed wireless channel model to the data-link layer using the cross-layer mapping. Finally, we show how to utilize classic methods of queuing theory to obtain performance characteristics of application running over the wireless channels.

1. Introduction

Up to date the Internet and wireless communications have been evolved as separate technologies because of different types of traffic they were intended for. With commercial launch of third generation (3G) networks, the convergence of these technologies is getting clear. Nowadays, we face the question of what a next generation (NG) mobile systems might or should be. Rather than linking NG to something like 'yet more bandwidth' at the air interface, the trend is to see NG as a new paradigm for wireless networks, mobile and fixed, where network and service characteristics of reconfigurability, interworking and adaptable services are the order of the day.

While NG mobile systems are not defined, there is a common agreement that these networks will rely on IP protocol as an end-to-end transport technology. The motivation is to introduce a unified service platform for future 'mobile Internet' known as NG All-IP network.

In addition to broadband wireless access to the Internet, NG All-IP networks must satisfy requirements of emerging QoS-aware applications. This is a problem for many service types even in fixed networks. Wireless and mobility issues add their own problems on top of this IP flaw. Time varying characteristics of wireless channels, teletraffic and mobility issues must be addressed before wireless Internet services will be commercially deployed. To facilitate development of these networks novel methods of teletraffic theory must be developed.

Large-scale propagation models developed to date [1–4] predict the received local average signal strength (RLASS) at a given distance from the transmitter and do not take into account rapid fluctuations of the signal strength. Small-scale propagation models [5–7] capture propagation characteristics of the wireless channels on a

finer granularity than large-scale ones and implicitly include the movement of the user up to the short travel distances. However, they fail to predict signal strength attenuation caused by movements over larger distances, e.g. between areas with different RLASS. Nevertheless, most performance evaluation studies of information transmission over wireless channels performed so far [8–11], were limited to small-scale propagation.

In this paper we propose an extension for existing wireless channel modeling techniques to the case of mobility-dependent behavior. The proposed model explicitly captures changes of propagation characteristics caused by movement of the user on the landscape integrating two different parts: mobility model and model of the wireless channel. Based on the amount of available information regarding a propagation environment we provide three parametrization methods. Then, we extend the proposed model to the data-link layer using the cross-layer mapping. To use the proposed model in performance evaluation studies we approximate the data-link wireless channel model by the artificial Markov modulated arrival process. To obtain performance characteristics of applications, we use this process together with arrival process modeling the traffic source as an input to the queuing system with non-preemptive priority discipline representing the service process of the wireless channel.

The paper is organized as follows. In Section 2 we review propagation characteristics and models used to capture them. In Section 3 we propose our wireless channel model. Parametrization methods are given in Section 4. In Section 5 we extend the model to small-scale propagation characteristics. Extension to the data-link layer is given in Section 6. Applications of the presented approach are outlined in Sections 7 and 8. Conclusions are drawn in the last section.

2. Propagation characteristics

The propagation path between the transmitter and a receiver may vary from simple line-of-sight (LOS) to very complex ones due to diffraction, reflection and scattering. To estimate performance of wireless channels, propagation models are often used. We distinguish between large-scale and small-scale propagation models [12].

The latter models focus on predicting the received local average signal strength (RLASS) over large separation distances between the transmitter and a receiver. Propagation models characterizing rapid fluctuations of the received signal strength over short time duration are called small-scale or fading models.

2.1. Large-scale propagation models

When a mobile user moves away from the transmitter over large distances the RLASS gradually decreases. This signal strength can be predicted using large-scale propagation models.

We distinguish between analytical and empirical large-scale propagation models. The former ones capture large-scale propagation based on analytical representation of physical phenomena. Empirical models are based on fitting analytical expressions to a set of measured data. The main advantage of these models is that they implicitly take into account all propagation factors, both known and unknown. Most large-scale propagation models assume that the RLASS decays as the power law function of the distance between the transmitter and a receiver.

There are a number of large-scale propagation models developed to date [1–4]. However, those models do not take into account movement of mobile users between areas with different values of RLASS.

2.2. Small-scale propagation models

When a mobile user moves over short distances the instantaneous received signal strength may vary rapidly. The reason is that the received signal is a sum of many components coming from different directions due to reflection, diffraction and scattering. Since phases, amplitudes and arriving times of components are random, the resulting signal may vary quickly and significantly.

To capture small-scale propagation characteristics we have to distinguish between two cases: there is a LOS between the transmitter and a receiver and there is no LOS. In presence of dominant non-fading component the small-scale propagation envelop distribution is Rician. As the dominant component fades away due to shadowing by obstacles the small-scale propagation envelop distribution degenerates to Rayleigh distribution.

Due to implicit incorporation of small-scale mobility in small-scale propagation models [5–7], most performance evaluation studies of information transmission over wireless channels performed so far [8–11], were limited to small-scale propagation phenomenon.

2.3. Mobility-dependent wireless channel modeling

During an active session a mobile user may change its location many times and these changes are not always

limited to short travel distances. Since movement of the user between areas with different RLASS and rapid fluctuations of the signal strength are not taken into account, wireless channel models developed to capture large-scale propagation phenomenon cannot be effectively used in performance evaluation studies.

Small-scale propagation models capture propagation characteristics on a finer granularity than large-scale ones and implicitly include the movement of the user up to the short travel distances. However, they fail to predict signal strength attenuation caused by movements over larger distances e.g., between areas with different RLASS. Novel wireless channel models must capture both movement of the user and small-scale propagation characteristics. Propagation characteristics must be considered as an explicit function of user's movement.

2.4. Cross-layer wireless channel modeling

Models of the received signal strength cannot be directly used in performance evaluation studies and must be properly extended to higher layers. Hence, we have to take into account characteristics of underlying layers including modulation schemes at the physical layer, data-link error concealment techniques and possible segmentation procedures between different layers. Finally, an adequate wireless channel model for performance evaluation studies must be cross-layer one capturing propagation characteristics of wireless channels as a mobility-dependent stochastic process and important properties of underlying layers. Such models along with traffic models have to be further applied to predict QoS expectations experienced by applications running over the wireless channels.

Cross-layer mobility-dependent design of the wireless channel model at the data-link layer is illustrated in the Fig. 1, where each layer is associated with appropriate stochastic process modeling the reception of protocol data units (PDU). Stochastic process at each layer is the complex cross-layer function of movement of the user, propagation characteristics and specific peculiarities of underlying layers.

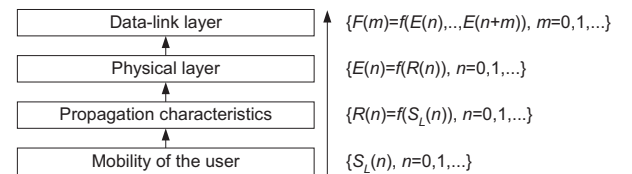


Figure 1. Cross-layer design of the wireless channel model.

3. Wireless channel model

3.1. Structure of the model

Assume that a given cell of a circular configuration with a single transmitter placed in the middle is divided into a finite number of areas M such that these areas are

non-overlapped and the sum of their areas equals to the area of the cell. We assume that a mobile user may arbitrary move between these areas and each area is associated with a certain value of RLASS. Several examples of the division of the cell into areas satisfying abovementioned assumptions are shown in the Fig. 2. In general, these areas may be of an arbitrary configuration.

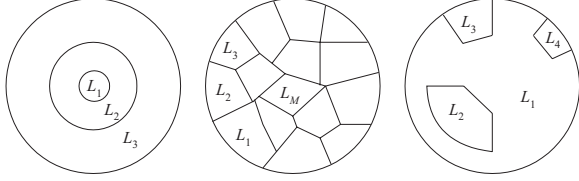


Figure 2. Examples of the division of the cell into areas.

Consider a discrete-time environment, i.e. time axis is slotted with a certain granularity Δt , the slot duration is constant and given by $\Delta t = (t_{i+1} - t_i)$, $i = 0, 1, \dots$. Assume that changes of areas are only allowed at the slot boundaries. Considering movement of the user between areas one may expect some type of positive autocorrelation in this process. Roughly speaking, if the user is in a certain area in the slot n it is more likely he will be in the same area in the slot $(n + 1)$. We propose to capture such type of positive autocorrelation representing the user movement between areas by the discrete-time homogenous Markov chain $\{S_L(n), n = 0, 1, \dots\}$, $S_L(n) \in \{1, 2, \dots, M\}$, where M is the number of areas. Let D_L be its transition probability matrix. According to this model, time, a particular user stays in each area is geometrically distributed. However, this restriction can be relaxed to capture more general distributions of sojourn times in each area, including sum of geometrical, hypergeometrical, etc. This can be done allowing more than one state of the Markov chain to denote each area.

In our model transitions are only allowed between adjacent areas that is a natural assumption regarding movement of the user within any given landscape. It is also possible to represent directional movement of the user introducing a periodicity in the Markov chain. For example, dealing with the highway scenario the sequence of areas visited by a mobile user may be known in advance.

The RLASS is the function of the distance between the transmitter and a receiver and movement of the user. To stochastically represent it, let us associate a certain value of RLASS with each state of the mobility model. To do so let $\{L(n), n = 0, 1, \dots\}$, $L(n) \in \{L_1, L_2, \dots, L_M\}$ be the doubly-stochastic RLASS process whose underlying Markov chain is $\{S_L(n), n = 0, 1, \dots\}$. Thus, the value of RLASS is modulated by the underlying Markov chain and the whole model is the doubly-stochastic process. Let $\vec{L} = (L_1, L_2, \dots, L_M)$ be the RLASS vector. Due to incorporation of Markovian modulating process the RLASS process is characterized by the following

structure of the autocorrelation function:

$$K_L(m) \sim \sum_{\forall l, l \neq 1} \lambda_l^m, \quad m = 1, 2, \dots, \quad (1)$$

where λ_l , $l = 2, 3, \dots, M$ are eigenvalues of the transition probability matrix of the Markov process $\{S_L(n), n = 0, 1, \dots\}$ given that $\lambda_1 \equiv 1$. Thus, the autocorrelation function of the RLASS process is the sum of $(M - 1)$ geometrically distributed terms given by non-unit eigenvalues of the modulating Markov chain.

3.2. Parametrization of the model

Our model is just a doubly-stochastic process. To completely define it we have to provide the transition probability matrix D_L and the RLASS vector \vec{L} .

Consider a cell of a circular configuration. Assume that the number of areas with appropriate values of RLASS, their configurations and boundaries between them are known. According to our model every area corresponds to the state of the Markov chain. It is straightforward to assume that the sojourn time in a certain area must depend on its size. Indeed, with the increasing of the size of the area, time, a user stays in this area is increasing. It is also crucial to take into account directional movement of users. For example, considering the highway scenario if a mobile user is in a certain area in the time slot n , it is more likely he will continue to the next area along the highway than move to any other area.

Consider a mobile user which is in the area i in the slot n . According to the proposed model, in the next slot $(n + 1)$ he may either stay in the area i or move to other area. The only areas to which a user can move in a one slot are adjacent areas denoted by Ω_i . Let us now consider areas from Ω_i as a single area adjacent to the area i . We propose to compute transition probabilities between area i and all those areas represented by Ω_i as follows:

$$\begin{cases} d_{L,i\Omega_i} = \frac{\sum_{\forall j \in \Omega_i} S_j}{S_R} \\ d_{L,ii} = \frac{S_i}{S_R} \end{cases}, \quad i = 1, 2, \dots, M, \quad (2)$$

where S_j is the area of area j , S_R is the area of the cell, $d_{L,i\Omega_i}$, $i = 1, 2, \dots, M$, are transition probabilities between the area i and all those areas from Ω_i . Depending on the length of the border between area i and areas from Ω_i transition probability $d_{L,i\Omega_i}$ must be distributed between transition probabilities $d_{L,ij}$, $j \in \Omega_i$, as follows:

$$d_{L,ij} = \frac{d_{i\Omega_i} V_{ij} w_{ij}}{\sum_{\forall j \in \Omega_i} V_{ij}}, \quad j \in \Omega_i, \quad (3)$$

where V_{ij} , $j \in \Omega_i$ are lengths of the borders between areas i and j . Parameters w_{ij} , $j \in \Omega_i$ are intended to represent directional movement of the user in a highway or urban scenarios. Since they are specific for a given environment, no general expression can be provided. However, note that:

$$\sum_{j \in \Omega_i} w_{ij} = 1, \quad i = 1, 2, \dots, M. \quad (4)$$

To complete parametrization, in the following section we consider how to determine the number of areas with appropriate values of RLASS, their configurations and boundaries between them using either measurements of RLASS or classic large-scale propagation models.

4. Estimation of parameters

4.1. Estimation based on measurements

In practise we cannot measure the value of RLASS in any point of the cell. Instead, measurements of RLASS are often represented by the following three-dimensional vector:

$$\vec{L}_{XY} = (x_i, y_i, L_i), \quad i = 1, 2, \dots, M, \quad (5)$$

where M is the number of measurements, (x_i, y_i) is the coordinate of the i^{th} measurement and L_i is the RLASS value of respective measurement.

Information given by $\vec{L}_{XY} = (x_i, y_i, L_i)$, $i = 1, 2, \dots, M$ are insufficient for our purposes. Indeed, to estimate parameters of our model using (2) and (3) we have to determine areas to which these measurements belong to. To determine areas with nearly the same RLASS we propose to use a suitable division of the cell into areas whose vertexes are measurement points.

In our case an appropriate division of the cell is achieved using the so-called Voronoi tessellation that separate a certain region D of space \mathbb{R}^n into polygons D_i , $i = 1, 2, \dots, M$, using the realization of a certain point process. The polygon D_i is the intersection of half planes H_{ij} bounded by the bisectors of the segments $((x_i, y_i), (x_j, y_j))$, $i, j = 1, 2, \dots, M$ and containing (x_i, y_i) as a vertex. Practically, for each measurement point (x_i, y_i) , $i = 1, 2, \dots, M$, D_i , $i = 1, 2, \dots, M$, is the area consisting of all locations in the space which are closer to (x_i, y_i) than to any other point. The system of all polygons forms a tessellation. In our case the space is \mathbb{R}^2 and coordinates of measurement points can be considered as the realization of a point process on \mathbb{R}^2 .

To ensure that the Voronoi tessellation is well defined the only requirement we have to impose on measurement points is that they must compose a non-degenerate realization of the point process. It means that there must be at least two measurement points, they are distinct, and there are only finitely many of these points in any bounded region. All these requirements are satisfied within our assumptions. There are a number of approaches to compute Voronoi tessellation (see [13] and references therein).

To determine the number of areas it is not strictly required to distinguish between every value of RLASS. Instead, it is possible to consider ranges of RLASS. In this case the range $(\max_{\forall i} L_i - \min_{\forall i} L_i)$ is divided into K non-overlapping ranges of the length:

$$\Delta L = \frac{(\max_{\forall i} L_i - \min_{\forall i} L_i)}{K}. \quad (6)$$

Using (6), all measurements must be classified to appropriate ranges and assigned the value of RLASS

corresponding to the middle of the appropriate range $(\min_{\forall i} L_i + k(\Delta L/2))$, $k = 1, 2, \dots, K$. Then, areas corresponding to these ranges can be determined using the procedure outlined below.

Let $l_{i,j}$, $i, j = 1, 2, \dots, M$, be the length between i^{th} and j^{th} measurement points and Ω_i be the set of areas adjacent to an arbitrary chosen area i . Assume that i^{th} measurement falls into k^{th} range of RLASS, i.e. the actual RLASS in the area i is $(\min_{\forall i} L_i + k(\Delta L/2))$. Choose the next measurement point such that the condition $\min_{j \in \Omega_i} l_{i,j}$, is satisfied. If this point falls into the the same range of RLASS these two areas can be considered together and assigned the same RLASS $(\min_{\forall i} L_i + k(\Delta L/2))$. The set Ω_i must now be redefined treating two areas that fall into the same range of RLASS as a single area. The same procedure must be subsequently performed for all measurement points from the new set Ω_i for which $\min_{j \in \Omega_i} l_{i,j}$ is satisfied until all points in Ω_i will be classified to other ranges of RLASS. Note that with the increasing of the range of RLASS the accuracy of the model may decrease.

An illustration of the proposed approach is shown in the Fig. 3, where the left figure shows measurement points on the plane, the Voronoi tessellation is shown next and the application of the classification algorithm is finally illustrated.

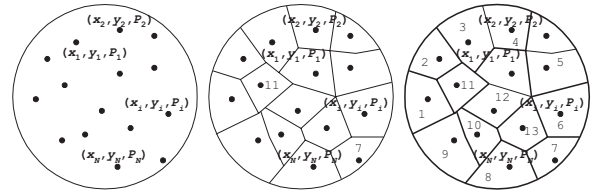


Figure 3. Measurement points on the plane (left), Voronoi tessellation (middle), resulting areas (right).

4.2. Estimation based on propagation models

Unfortunately, measurements of RLASS are often unavailable while basic characteristics of a given environment are known. In this case it is possible to determine the number of areas, their configurations, boundaries and the RLASS vector based on classic large-scale propagation models developed to date.

Most of large-scale propagation models assume that with the increasing of the distance between the transmitter and a receiver d , RLASS is decreasing according to a power law of d :

$$L(d) \sim \left(\frac{d}{d_0}\right)^n. \quad (7)$$

where n is the pass loss exponent, d_0 is the standard distance. Distance d_0 is often assumed to be 1000 meters for macrocells, 100 meters for microcells and 1 meter for indoor wireless channels [12]. For example, free space propagation model assumes that there is only one unobstructed LOS path between the transmitter and a receiver.

The free space propagation loss is then given by:

$$U(d) = U_s(d_0) + 20 \lg \left(\frac{d}{d_0} \right), \quad (8)$$

where $U_s(d_0)$ is the propagation loss at the standard distance. $U_s(d_0)$ can be measured or approximated [12].

It rarely occurs in practice that the LOS is unobstructed. As a result, the estimation given by (8) fails in most cases. Indeed, using measurements Okumura *et al.* [3] have shown that with the increasing of the distance between the transmitter and a receiver, propagation loss is rarely decreasing at a rate with $n = 2$. Hata [14] fits propagation curves to empirical formulas and determined that the propagation loss is proportional to the separation distance as:

$$E[U(d)] = U_s(d_0) + 10n \lg \left(\frac{d}{d_0} \right). \quad (9)$$

The path loss exponent n depends on the wavelength, antenna height and a given propagation environment. For example, if we take an assumption of free space propagation $n = 2$ and (9) degenerates to (8). When the LOS is shadowed $n > 2$. Considering urban areas, in certain circumstances $n < 2$ (see [12] for a range of n for specific environments). Additionally, measurements carried out by Seidel *et al.* [15] have shown that the actual propagation loss may vary significantly from the mean given by (9). Particularly, it was found that the actual value of propagation loss $U(d)$ is log-normally distributed with mean $E[U(d)]$. Finally, the expression for propagation loss $U(d)$ in a particular environment is given by:

$$U(d) = U_s(d_0) + 10n \lg \left(\frac{d}{d_0} \right) + X_\sigma, \quad (10)$$

where $X_\sigma \sim N(0, \sigma^2)$ is zero-mean Gaussian distributed random variable expressed in dB. The value of X_σ can be estimated from measurements for different locations of the transmitter and a receiver. Usually, $X_\sigma \in \{6 - 10\}$ dB. Given a certain transmitted power the propagation loss can be related to RLASS [12].

Using abovementioned considerations we assume that the areas with different RLASS are given by circles with different radiuses as shown in the left part of the Fig. 2. The range of RLASS in every area can be estimated using (10), while (8) can be seen as a rough approximation. Finally, D_L can be found using (2) and (3).

4.3. Estimation based on shadow configurations

The pass loss exponent n may vary significantly depending on the presence, density and configuration of shadowers in a given propagation environment. We took it into account introducing a deviation parameter X_σ that depends on a given environment and must be estimated from measurements of the signal strength. However, in those environments where shadowers are rare this may lead to significant modeling errors due to large deviation of n within a single area of a circular form. Thus, the assumption of circular configuration of areas with nearly

the same RLASS may no longer hold. To avoid it, in what follows, we introduce the model of RLASS based on direct estimation of shadowed and non-shadowed areas.

Assume that the centers of shadowers are Poissonially distributed on the plane with a certain finite intensity λ . The parameter λ determines the mean density of points and must depend on a given landscape. For example, if we consider the urban environment λ must be high while dealing with the highway or country-side scenarios λ is generally low. Poisson assumption allows to avoid detailed geographical description of the landscape while improve the accuracy of the model explicitly taking into account the presence of shadowers. Moreover, the Poisson assumption can be relaxed, if necessary. For example, Markov random field can be used instead.

To proceed further we take the following assumptions regarding a propagation environment and configuration of shadowers:

- all shadowers are of rectangular form;
- thickness of shadowers is zero;
- width of shadowers is arbitrary distributed;
- height of shadowers is arbitrary distributed;
- height of transmitter antenna h_a is known.

Consider three possible shadow placements caused by shadowers with different relation between initial parameters shown in Fig. 4, where d_s is the maximum shadow length, R is the radius of the cell, d is minimal distance between the center of the cell and shadower and h_s is the height of shadower. Depending on the relation between R , d , h_a and h_s we have to distinguish between three cases:

- $h_a > h_s, d_s \leq R - d$: the shadow is bounded in the cell;
- $h_a > h_s, d_s > R - d$: the shadow continues up to the border of the cell and bounded outside the cell;
- $h_a < h_s$: the shadow continues up to the border of the cell and virtually unbounded.

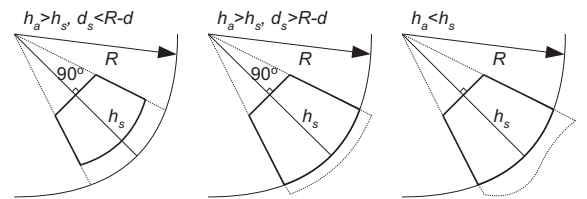


Figure 4. Possible placements of the shadow in a given cell.

Since we restricted our attention to only one cell, the latter two case are similar and can be treated simultaneously. Let us firstly determine the area of the shadow

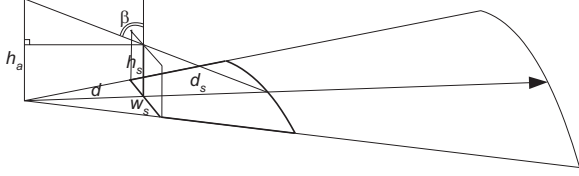


Figure 5. An illustration of shadowed area: $h_a > h_s, d_s \leq R - d$.

shown in the left part of the Fig. 4. Consider a different view of the same shadow presented in the Fig. 5.

Using simple geometric identities the length of the shadow d_s is expressed via initial parameters as follows:

$$d_s = \frac{h_s}{\cot \beta}, \quad h_a > h_s, \quad d_s \leq R - d, \quad (11)$$

where

$$\beta = 90^\circ - \arctan \frac{d}{h_a - h_s}. \quad (12)$$

Taking into account two other cases the final expression for d_s is given by:

$$d_s = \min \left(\frac{h_s}{\cot \beta}, R - d \right). \quad (13)$$

Using (24) the area of the shadow is now given by:

$$S_s = \min(S_{d_s}, S_{R-d}), \quad (14)$$

where S_{d_s} is the area of the segment with radius $(d + d_s)$ except for the area of the triangle with height d , S_{R-d} is the area of the segment with radius R except for the area of the triangle with height d .

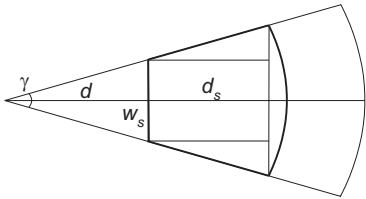


Figure 6. An illustration of shadowed area: $h_a > h_s, d_s \leq R - d$.

To determine the area of the shadow let us now consider the Fig. 6. The area of the shadow is given by:

$$S_{d_s} = 4\pi(d + d_s)^2 \frac{\gamma}{360} - \frac{dw_s}{2}. \quad (15)$$

For those cases when $h_a > h_s, d_s > R - d$ or $h_a < h_s$ the area is given by:

$$S_{R-d} = 4\pi R^2 \frac{\gamma}{360} - \frac{dw_s}{2}. \quad (16)$$

Finally, the area of the shadow is expressed as:

$$S_s = \min \left(\frac{4\pi R^2 \gamma}{360}, \frac{4\pi(d + d_s)^2 \gamma}{360} \right) - \frac{dw_s}{2}. \quad (17)$$

The same estimation must be performed for all other shadowers obtained via realizations of the Poisson process with intensity λ and random variables corresponding to widths and heights of shadowers. However, one may note that the overlapping of shadows may occur. In this case the estimation of the shadowed areas is more complicated but still feasible.

For every shadowed area the range of RLASS can now be estimated using the Hata-Seidel model (10) with $n > 2$. For unshadowed areas $n \approx 2$. However, there can be shadows whose length d_s is only insignificantly less than the radius of the cell R . Thus, the range of RLASS corresponding to this shadow can be very large leading to significant modeling errors. To avoid it, in addition to division of the cell into shadowed and non-shadowed areas we propose to divide the cell into circles with different radius to which shadows must be further classified as shown in the Fig. 7. New shadowed and non-shadowed areas are now given by borders of these circles and borders of shadows. Thus, we get areas with different RLASS where shadows are completely or partially within the different circles. Finally, the transition probabilities between these areas can be found using (2) and (3).

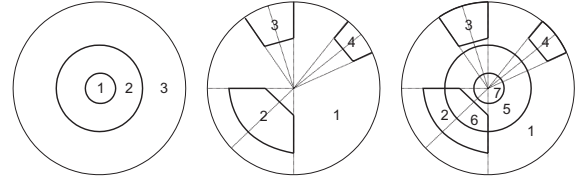


Figure 7. Division of the cell into circular areas (left), division of the cell into shadowed and non-shadowed areas (middle), resulting areas.

5. Extension to the small-scale propagation

Large-scale propagation models capture propagation characteristics on a coarse granularity using only the first moment of the received signal strength process. It is known that the received signal strength may vary rapidly causing frequent bit errors even when the average channel 'conditions' are good. As a result, large-scale propagation models cannot be effectively used in performance evaluation of applications running over wireless channels and must be seen as rough approximations. Small-scale propagation models capture propagation characteristics of the wireless channel on a finer granularity than large-scale ones [5,7], and thus, they are better suited for performance evaluation studies.

Small-scale propagation characteristics in a certain area are often modeled by the doubly-stochastic process $\{R_i(n), n = 0, 1, \dots\}$ modulated by the discrete-time Markov chain $\{S_{R,i}(n), n = 0, 1, \dots\}$, $S_{R,i}(n) \in \{1, 2, \dots, H\}$, each state of which is associated with conditional probability distribution function of the received signal strength $F_{R,i}(k|\Delta f|j)(\Delta f) = Pr\{R_i(n) =$

$k\Delta f|S_{R,i}(n) = j$, $k = 1, 2, \dots, N$, $j = 1, 2, \dots, H$, where N is the number of bins to which the signal strength is partitioned, Δf is the discretization interval [16,17]. Underlying modulation allows to take into account autocorrelation properties found in the received signal strength process. In what follows, we use $F_{R,i}(k|j)$ instead of $F_{R,i}(k\Delta f|j)(\Delta f)$.

To capture small-scale propagation characteristics of wireless channels we have to distinguish between two cases: there is a LOS between the transmitter and the receiver and there is no LOS. In presence of the dominant non-fading component the small-scale propagation envelop distribution is Rician. As the dominant component fades away due to shadowing by obstacles the small-scale propagation envelop distribution degenerates to Rayleigh one. Thus, the marginal distribution in an arbitrary area is either Rayleigh or Rician. Additionally, according to previously defined large-scale propagation model every area of the cell is associated with different RLASS. As a result, small-scale propagation characteristics in different areas are, at least, qualitatively (different RLASS) or quantitatively (different distributions) different. Therefore, every area i , $i = 1, 2, \dots, M$, must be associated with an unique small-scale propagation model $\{R_i(n), n = 0, 1, \dots\}$, $i = 1, 2, \dots, M$ such that $E[R_i] = L_i$, i.e. the RLASS of the area i is the mean of the stochastic process $\{R_i(n), n = 0, 1, \dots\}$. We also require that the state space of all small-scale propagation models is the same and given by $S_{R,i}(n) \in \{1, 2, \dots, H\}$, $i = 1, 2, \dots, M$.

We choose the slot duration Δt of the small-scale propagation models such that it equals to the time to transmit a single bit at the wireless channel.¹ Hence, the choice of Δt explicitly depends on properties of the physical layer. Since it is allowed for $\{S_R(n), n = 0, 1, \dots\}$ to change its state in every slot, every bit may experience different signal strengths.

Let us now integrate the small-scale propagation models to the mobility model. According to our assumptions small-scale propagation characteristics must be probabilistic function of the user's movement between areas:

$$S_R(n) = f_{Pr}(S_L(n) \in \{1, 2, \dots, M\}), \quad (18)$$

where $S_R(n)$ is the state of the underlying Markov chain $\{S_R(n), n = 0, 1, \dots\}$ of mobility-dependent small-scale propagation model $\{R(n), n = 0, 1, \dots\}$, index Pr denotes probabilistic relationship. Thus, the choice of small-scale propagation model $\{R_i(n), n = 0, 1, \dots\}$, $i = 1, 2, \dots, M$ must depend on the current area i :

$$S_R(n) = \begin{cases} S_{R,1}(n), & S_L(n) = 1, \\ \dots & \dots \\ S_{R,M}(n), & S_L(n) = M. \end{cases} \quad (19)$$

Given that all small-scale propagation models associated with states of the mobility model have the same number of states H , the state-space of

¹Note that the slot durations of the mobility model and small-scale propagation model must be equal and synchronized.

$\{S_R(n), n = 0, 1, \dots\}$ can now be defined as $S_R(n) \in \{(1, 1), \dots, (2, 1), \dots, (M, 1), \dots, (M, H)\}$, where the first index denotes the state of the mobility model, the second one is the state of the corresponding small-scale propagation model. Despite of the double description of the state, we still deal with one dimensional Markov chain. To show it we can re-enumerate the state space of the resulting model. However, state description given by (i, j) , $i \in \{1, 2, \dots, M\}$, $j \in \{1, 2, \dots, H\}$, is more convenient and reminds that the whole model is a special superposition of the mobility and propagation models.

Considering (19), it is clear that an appropriate small-scale propagation model must only be associated with the state of the mobility model corresponding to the appropriate area. Hence, the choice of transition probabilities of the mobility-dependent small-scale propagation model must depend on the state of the mobility model:

$$d_{R,lm} = \begin{cases} d_{R,1,lm}, & S_L(n) = 1, \\ \dots & \dots \\ d_{R,M,lm}, & S_L(n) = M. \end{cases} \quad (20)$$

where $d_{R,lm}$, $l, m \in \{1, 2, \dots, H\}$, $i \in \{1, 2, \dots, M\}$ are different as far as they belong to transition probability matrices of different Markov chains. Then, the transition probability matrix D_R of the of the integrated model is given by the following product:

$$\begin{pmatrix} d_{L,11}D_{R,1} & \dots & d_{L,1M}D_{R,M} \\ d_{L,21}D_{R,1} & \dots & d_{L,2M}D_{R,M} \\ \vdots & \ddots & \vdots \\ d_{L,M1}D_{R,1} & \dots & d_{L,MM}D_{R,M} \end{pmatrix}, \quad (21)$$

where $d_{L,ij}$, $i, j = 1, 2, \dots, M$, are transition probabilities of the mobility model, $D_{R,i}$, $i = 1, 2, \dots, M$, are transition probability matrices of $\{S_{R,i}(n), n = 0, 1, \dots\}$.

The proposed small-scale mobility-dependent propagation model is simply a probabilistic function of the Markovian model representing the user's movement between areas with different propagation characteristics. Thus, the whole model can be seen as a triply stochastic process while does not lead outside hidden Markov model. To completely define the mobility-dependent small-scale propagation model we must provide $D_{R,i}$, $F_{R,i}(k|j)$, $i = 1, 2, \dots, M$, $k = 1, 2, \dots, N$, $j = 1, 2, \dots, H$.

5.1. Parametrization based on measurements

Given M and \vec{L} parameters of the small-scale propagation models $D_{R,i}$, $F_{R,i}(k|j)$, $i = 1, 2, \dots, M$, $k = 1, 2, \dots, N$, $j = 1, 2, \dots, H$, can be estimated using measurements of the small-scale propagation characteristics as outlined in [16,17].

5.2. Histogram matching method

Measurements of the small-scale propagation characteristics are often unavailable. In this case we propose to parameterize the small-scale propagation models us-

ing the histogram matching method. Indeed, depending on the presence of LOS in the area i stochastic process $\{R_i(n), n = 0, 1, \dots\}$ must have either Rician or Rayleigh marginal distributions with mean $E[R_i] = L_i$. Setting $H = 1$, Rayleigh or Rician distribution can be represented via histograms with frequency densities defined as follows:

$$F_{R,i}(k|j) = \frac{p_k}{x_{k+1} - x_k},$$

$$p_k = \int_{x_k}^{x_{k+1}} f_X(x) dx, \quad (22)$$

where $f_X(x)$ is Rayleigh or Rician distribution.

The discrete nature of $\{R_i(n), n = 0, 1, \dots\}$ does not restrict generality of the model. Indeed, given $\Delta f \rightarrow 0$ the marginal probability distribution function of $\{R_i(n), n = 0, 1, \dots\}$ tends to Rayleigh or Rician distribution. We can always choose Δf so small that this condition is satisfied. Therefore, setting $H = 1$ we can capture distributional properties of the received signal strength process with any given accuracy.

6. Extension to the data-link layer

The small-scale propagation model of the received signal strength cannot be directly used in performance evaluation studies of protocols or information transmission at different layers, and thus, must be previously extended to those layers. To do so we have to take into account specific peculiarities of underlying layers including modulation schemes at the physical layer, data-link error concealment methods and segmentation procedures between different layers.

In the following subsections we propose an extension of the mobility-dependent small-scale propagation model to the data-link layer. Particularly, we define models of incorrect reception of PDUs at different layers. For this purpose we implicitly assume that appropriate PDUs are consecutively transmitted at corresponding layers.

6.1. Bit error process

Consider an arbitrary state i of the Markov chain $\{S_R(n), n = 0, 1, \dots\}$ associated with conditional probability distribution function $F_L(k|i)$, $k = 1, 2, \dots, N$, of the received signal strength. Since the probability of the single bit error is the deterministic function of the received signal strength [12], all values of $F_R(k|i)$ that are less or equal to a computed value of the so-called bit error threshold B_T cause bit error. Those values which are greater than B_T do not cause bit error. Thus, each state of the Markov process $\{S_R(n), n = 0, 1, \dots\}$ can be associated with the following bit error probability $p_{E,i}$:

$$p_{E,i} = Pr\{E(n) = 1 | S_E(n) = i\} =$$

$$= \sum_{k=1}^{B_T} Pr\{R(n) = k | S_R(n) = i\}, \quad (23)$$

where $\{E(n), n = 0, 1, \dots\}$, $E(n) \in \{0, 1\}$ is the bit error process for which 1 denotes the incorrectly received

bit, 0 denotes the correctly received bit, $\{S_E(n), n = 0, 1, \dots\}$ is the underlying Markov chain of $\{E(n), n = 0, 1, \dots\}$. Note that $\{S_R(n), n = 0, 1, \dots\}$ and $\{S_E(n), n = 0, 1, \dots\}$ are the same and $\vec{\pi}_E = \vec{\pi}_R$, $D_E = D_R$, where D_E and $\vec{\pi}_E$ are the one-step transition probability matrix and the stationary distribution vector of $\{S_E(n), n = 0, 1, \dots\}$ respectively. B_T must be estimated based on the modulation scheme and other specific features of the physical layer utilized at the wireless channel [12].

Let us denote by $d_{E,ij}(k) = Pr\{E(n) = k, S_E(n) = j | S_E(n-1) = i\}$, $k = 0, 1$, the transition probability from the state i to the state j with correct and incorrect bit reception respectively. These probabilities can be represented in a compact form using matrices $D_E(1)$ and $D_E(0)$ such that $D_E(1) + D_E(0) = D_E$. In our case the state from which the transition occurs completely determines the bit error probability. The state to which transition occurs is used for convenience of matrix notation.

6.2. Frame error process without FEC

Assume that the length of the frame is constant and equals to m bits. Sequence of consecutively transmitted bits, denoted by gray rectangles, is shown in the Fig. 8, where $(l-1)$, l , $(l+1)$ denote time intervals whose length equals to the time to transmit exactly one frame at the wireless channel; k , i , j , denote the state of $\{S_E(n), n = 0, 1, \dots\}$ in the beginning of these time intervals.

Consider the stochastic process $\{N(l), l = 0, 1, \dots\}$, $N(l) \in \{0, 1, \dots, m\}$, describing the number of incorrectly received bits in consecutive bit patterns of the length m . This process is doubly stochastic one with underlying Markov chain $\{S_N(l), l = 0, 1, \dots\}$ and can be completely defined via parameters of the bit error process.

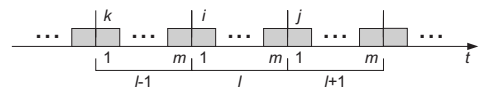


Figure 8. Consecutively transmitted bits at the wireless channel.

Let us denote the probability of going from the state i to the state j for the Markov chain $\{S_N(l), l = 0, 1, \dots\}$ with exactly k , $k = 0, 1, \dots, m$ incorrectly received bits in a bit pattern of the length m by $d_{N,ij}(k) = Pr\{N(l) = k, S_N(l) = j | S_N(l-1) = i\}$. These probabilities can be found using $D_E(k)$, $k = 0, 1, \vec{\pi}_E$:

$$d_{N,ij}(0) = \vec{\pi}_E D_E^m(0) \vec{e},$$

$$d_{N,ij}(1) = \vec{\pi}_E \sum_{k=m-1}^0 D_E^{m-k-1}(0) D_E(1) D_E^k(0) \vec{e},$$

$$\dots$$

$$d_{N,ij}(m) = \vec{\pi}_E D_E^m(1) \vec{e}, \quad (24)$$

where \vec{e} is the vector of ones of appropriate size.

Let us now introduce the frame error process $\{F(l), l = 0, 1, \dots\}$, $F(l) \in \{0, 1\}$, where 0 indicates the correct frame reception, 1 denotes the incorrect frame reception. Process $\{F(l), l = 0, 1, \dots\}$ is modulated by the underlying Markov chain $\{S_F(l), n = 0, 1, \dots\}$. Note that $\{S_F(l), l = 0, 1, \dots\}$ and $\{S_N(l), l = 0, 1, \dots\}$ are the same. Let us denote the probability of going from the state i to the state j for the Markov chain $\{S_F(l), l = 0, 1, \dots\}$ with exactly k , $k = 0, 1$ incorrectly received frames by $d_{F,ij}(k)$. Process $\{N(l), l = 0, 1, \dots\}$ describing the number of bit errors in the consecutive frames can be related to the frame error process $\{F(l), l = 0, 1, \dots\}$ using the so-called frame error threshold F_T :

$$\begin{aligned} d_{F,ij}(0) &= \sum_{k=0}^{F_T-1} d_{N,ij}(k), \\ d_{F,ij}(1) &= \sum_{k=F_T}^m d_{N,ij}(k). \end{aligned} \quad (25)$$

Expressions (25) are interpreted as follows: if the number of incorrectly received bits in the frame is greater or equal to a computed value of the frame error threshold ($k \geq F_T$) the whole frame is incorrectly received and $F(l) = 1$, otherwise ($k < F_T$) frame is correctly received and $F(l) = 0$.

Assume that FEC is not used at the data-link layer. It means that every time a frame contains at least one bit error, it is received incorrectly ($F_T = 1$). Thus, the transition probabilities (25) of the frame error process take the following form:

$$\begin{aligned} d_{F,ij}(0) &= d_{N,ij}(0), \\ d_{F,ij}(1) &= \sum_{k=1}^m d_{N,ij}(k) = 1 - d_{F,ij}(0). \end{aligned} \quad (26)$$

The slot durations of $\{N(l), l = 0, 1, \dots\}$ and $\{F(l), l = 0, 1, \dots\}$ are the same $\Delta t'$ and related to the slot duration of received signal strength process $\{L(n), n = 0, 1, \dots\}$ as $\Delta t' = n\Delta t$, $n = 0, 1, \dots$.

6.3. Frame error process with FEC

F_T depends on FEC correction capabilities. Assume that the number of bit errors that can be corrected by a FEC code is l . Then, $F_T = (l + 1)$ and a frame is incorrectly received when $k \geq (l + 1)$. Otherwise, it is correctly received. Thus, the transition probabilities (25) of the frame error process take the following form:

$$\begin{aligned} d_{F,ij}(0) &= \sum_{k=0}^l d_{N,ij}(k), \\ d_{F,ij}(1) &= \sum_{k=l+1}^m d_{N,ij}(k). \end{aligned} \quad (27)$$

6.4. Illustration of the proposed extension

An illustration of the proposed cross-layer mapping is shown in the Fig. 9, where time diagrams of $\{R(n), n =$

$0, 1, \dots\}$, $\{E(n), n = 0, 1, \dots\}$, $\{N(l), l = 0, 1, \dots\}$ and $\{F(l), l = 0, 1, \dots\}$ are shown. Error thresholds B_T and F_T must be estimated as outlined previously and then used to compute transition probabilities of error processes at different layers.

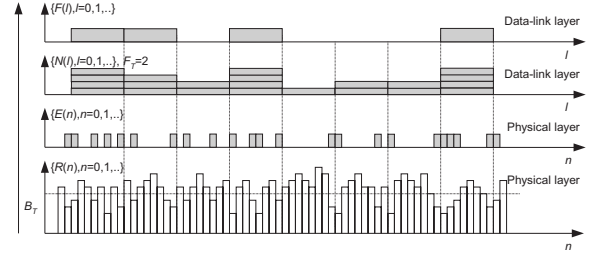


Figure 9. An illustration of the proposed cross-layer mapping.

7. Applications

To define models of the incorrect reception of PDUs at different layers we implicitly assumed that the appropriate PDUs are consecutively transmitted at corresponding layers. Hence, the frame error process is conditioned on the event of consecutive transmission of frames. Considering wireless channel and teletraffic models jointly we remove such a conditioning and obtain a single stochastic process representing the frame service process at the wireless channel. This process has two outcomes at any time slot: is the frame generated or not and, if generated, is the frame correctly received or not. If the traffic model is Markovian in nature both simulation and analytic studies can be performed.

According to the simulation approach, we have to synchronize the traffic model and the data-link layer wireless channel model. Then, the performance parameters of interest can be directly derived. In the upper part of Fig. 10 example of loss trace is shown. This approach is suitable when only FEC is used at the data-link layer.

According to the analytic approach, we must replace the data-link layer wireless channel model by an artificial equivalent arrival process using error/arrival mapping as shown in Fig. 10. The mapping is straightforward: every slot when the frame is incorrectly received with a certain probability, an arrival occurs with the same probability. Thus, the structure and parameters of the process remains unchanged. Then, the artificial arrival process and arrival process from the traffic source must be used as an input to the queuing system with appropriate priority service discipline representing the frame service process at the wireless channel. In this model arrivals from artificial arrival process must be of higher priority than those from arrival process modeling the traffic source. Depending on the parameters of the queuing system different data-link operations can be modeled. In general, analytical approach allows to get exact results when FEC is used at the data-

link layer and approximate values of performance parameters when ARQ or hybrid ARQ/FEC is used.

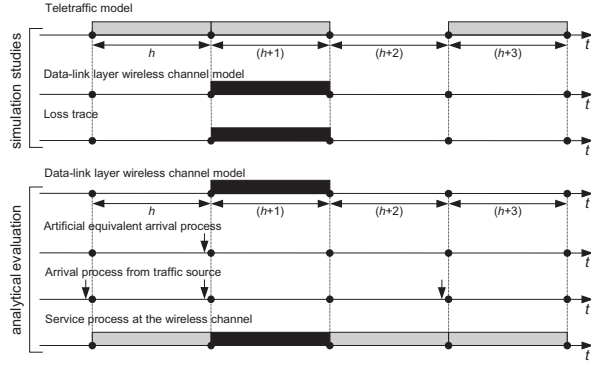


Figure 10. An illustration of simulation and analytic studies.

Both described approaches do not capture exact performance of ARQ protocols. Indeed, high functional complexity combined with non-zero round trip times and unreliable feedback restricts their precise analytical modeling. However, using our data-link layer wireless channel model it is still possible to derive performance parameters implementing simulation studies. For these studies our approach provides a modular structure of the modeling environment, thus, eliminating the need for computationally expensive simulations at the physical layer. Indeed, the simulation algorithm may consist of three basic blocks: data-link layer wireless wireless channel model, teletraffic model and ARQ logic.

8. Example of the analytic study

8.1. Artificial arrival process

Given a Markov chain each state of which is associated with a certain frame error probability we propose to approximate the complexity of the frame error process by a so-called 'artificial' Markov modulated arrival process using error/arrival mapping. An illustration of mapping is shown in the Fig. 11, where time diagrams of data-link layer wireless channel model and corresponding artificial arrival process are shown, black rectangles denote incorrect frame reception, arrows indicate arrivals. Since it is not required to change the Markovian structure and parameters of the data-link layer wireless channel model, new parametrization procedure is not needed. The resulting arrival process is classified as a discrete-time Markovian arrival process (D-MAP), denoted by MAP_E .

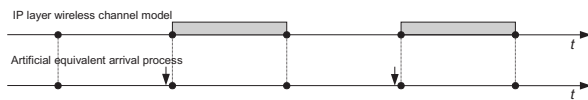


Figure 11. An illustration of error/arrival mapping.

8.2. Tagged arrival process

Assume that the arrival process from the traffic source is represented by D-MAP $\{W_T(n), n = 0, 1, \dots\}$ with the underlying Markov chain $\{S_T(n), n = 0, 1, \dots\}$, $S_T(n) \in \{1, 2, \dots, M_T\}$. According to it, each pair of states of the set $\{1, 2, \dots, M_T\}$ is associated with probability of one arrival, i.e. given a pair (i, j) , $i, j = 1, 2, \dots, M_T$ one arrival occurs in a slot with probability $p_{T,ij} = Pr\{W_T(n) = 1, S_T(n) = i | S_T(n-1) = i\}$ and no arrival occurs with complementary probability $(1 - p_{T,ij})$. We denote this process by MAP_T .

D-MAP is a quite versatile arrival process that can be used to model arrival processes from the different traffic sources. Extensions to more complicated arrival processes (e.g., batch D-MAP) are also possible. The only restriction is that the process must have an underlying Markovian structure.

8.3. Description of the queuing system

Assume that every arrival requires a service time of exactly one slot. The slot duration is constant and equal to the time to transmit one frame at the wireless channel $\Delta t'$. Since we limit ourselves to only one traffic source this assumption is not restrictive. The queuing system satisfying abovementioned assumption is represented as $MAP_T + MAP_E / D / 1 / K$ where arrivals from MAP_E are of higher priority than those from MAP_T .

The system operates as follows. At each slot boundary the server tries to serve an arrival from MAP_E , if any. If not, it serves an arrival from MAP_T , if any. Since arrivals from both processes may only occur at the slot boundaries, to emulate the preemption of arrivals from the traffic source it is sufficient to assume a non-preemptive priority discipline. Indeed, any arrival coming from MAP_E is scheduled for the service at the beginning of the nearest slot. Since at most one arrival may occur per a slot from MAP_E these arrivals do not wait for service. As a result, waiting positions are only occupied by low priority arrivals from MAP_T . The service discipline is FCFS for low priority arrivals.

Setting the number of waiting positions to zero we obtain the model that assumes only FEC at the data-link layer. Indeed, since only those arrivals coming from MAP_E can be lost, loss can be interpreted as an unsuccessful reception of the frame.

Setting the number of waiting positions to a non-zero value we approximate the performance of ARQ protocol at the data-link layer. Indeed, every time when a frame cannot be successfully received, another frame arrives from artificial equivalent arrival process and transmitted instead. Thus, the transmission of the frame from the traffic source is postponed for a service time of an arrival with high priority and can be interpreted as an unsuccessful transmission of the frame. If characteristics of the wireless channel are such that no arrival from artificial equivalent arrival process is available, the postponed frame is scheduled for transmission at the beginning of the next slot. The additional assumption we have to take is that the receiver knows whether the transmission of the

frame is successful or not at the end of the transmission of the frame i.e., the feedback is instantaneous and perfect.

8.4. Queuing analysis

The loss probability is an important parameter for loss and delay/loss sensitive applications. Given previously defined queuing model we have to determine frame losses experienced by MAP_T due to buffer overflows.

Time diagram of the queuing system is given in the Fig. 12. Complete description of the queuing system requires a two-dimensional Markov chain $\{S_A(n), S_Q(n), n = 0, 1, \dots\}$ embedded at the moments of departures, where $S_A(n) = S_E(n) \times S_T(n)$ is the state of superposition of MAP_T and MAP_E , $S_Q(n) \in \{0, 1, \dots, K\}$ is the number of customers in the system at the moments of departures. Let T be the transition matrix of such Markov chain and $\vec{x} = (x_{1,0}, \dots, x_{M_A, K})$, $M_A = M_E M_T$ be the row array containing stationary probabilities. One can solve for \vec{x} using $\vec{x}T = \vec{x}$, $\vec{x}\vec{e} = 1$.

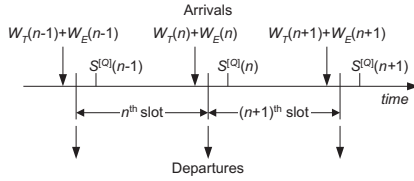


Figure 12. Time diagram of the queuing system.

The mean arrival rate of processes to the queuing system is given by:

$$\begin{aligned} E[W_T] &= \sum_{i=1}^{M_T} \pi_{T,i} \sum_{j=1}^{M_T} p_{T,ij}, \\ E[W_E] &= \sum_{i=1}^{M_E} \pi_{E,i} \sum_{j=1}^{M_E} p_{E,ij}, \end{aligned} \quad (28)$$

where $\pi_{T,i}$ and $\pi_{E,i}$ are elements of the stationary probability vectors of $\{S_T(n), n = 0, 1, \dots\}$ and $\{S_E(n), n = 0, 1, \dots\}$ respectively, $p_{T,ij}$, $i, j = 1, 2, \dots, M_T$ are probabilities of arrival from $\{W_T(n), n = 0, 1, \dots\}$ going from state i to state j , $p_{E,ij}$, $i, j = 1, 2, \dots, M_E$ are probabilities of arrival from $\{W_E(n), n = 0, 1, \dots\}$ going from state i to state j .

An important observation comes directly from (28). Assume an infinitely large buffer space. Then, for the system to be stable we must require $E[W_T] + E[W_E] < 1$. However, MAP_E is just a representation of wireless channel characteristics; only one arrival per a slot is possible for this process and these arrivals always seize the server. Therefore, the system is always stable for MAP_E . However, it may be the case that $E[W_T] + E[W_E] \geq 1$, and the system is not stable for arrival process modeling the traffic source. As a result, the service represented by the MAP_T may not operate stably in a given environment.

Let us now assume that the number of waiting positions is limited and determine the loss probability L_T for

MAP_T as a limiting probability of the ratio between the number of lost arrivals of MAP_T in a slot and the number of arrivals from this process in a slot:

$$L_T = \lim_{n \rightarrow \infty} \frac{L_T(n)}{W_T(n)}. \quad (29)$$

Since at most one arrival is allowed in a slot from each arrival process the loss of arrival from MAP_T (low priority process) always occurs when the state of the queuing system is $(S_A = i, S_Q = K)$, $i = 1, 2, \dots, M_E M_T$ and may occur when the state of the system is $(S_A = i, S_Q = K - 1)$. We have:

$$\begin{aligned} L_T(n) &= \sum_{i=1}^{M_E} \sum_{j=1}^{M_T} x_{(i,j), K} \sum_{l=1}^{M_T} p_{T,jl} + \\ &+ \sum_{j=1}^{M_E} \sum_{i=1}^{M_T} x_{(i,j), K-1} \sum_{m=1}^{M_E} p_{E,im} \sum_{l=1}^{M_T} p_{T,jl}. \end{aligned} \quad (30)$$

where $x_{(i,j), K}$ and $x_{(i,j), K-1}$ are $(i + j, K)$ and $(i + j, K - 1)$ elements of stationary distribution of $\{S_A(n), S_Q(n), n = 0, 1, \dots\}$.

The number of arrivals from MAP_T in a slot is given by (28). Substituting (28) and (30) to (29) we get a final expression for loss probability.

Let us now determine mean performance parameters. Denote by $E[S_{T,Q}]$, $E[S_{E,Q}]$ and $E[S_{A,Q}]$ the mean number of customers in the system of MAP_T , MAP_E and superposed arrival processes respectively. For these quantities the following simple relation holds:

$$E[S_{T,Q}] = E[S_{A,Q}] - E[S_{E,Q}]. \quad (31)$$

Since MAP_E has an absolute priority over MAP_T , $E[S_{T,Q}]$ can be estimated from the queuing system $\text{MAP}_E/D/1/K$ neglecting those arrivals coming from MAP_T . For arrivals from MAP_E in $\text{MAP}_E/D/1/K$ queuing system the Little's result gives:

$$E[S_{E,Q}] = E[W_E]E[D_E], \quad (32)$$

where $E[D_E]$ is the mean sojourn time (in the system) of arrivals from MAP_E . One may note that this time is always equal to the service time (one slot). Indeed, at most one arrival from MAP_E is allowed and this arrival is always served without waiting for service (high priority process). Therefore, we have:

$$E[S_{E,Q}] = \sum_{i=1}^{M_E} \pi_{E,i} \sum_{j=1}^{M_E} p_{E,ij}, \quad (33)$$

where $\pi_{E,i}$ is the i^{th} element of steady-state distribution of $\{S_E(n), n = 0, 1, \dots\}$.

$E[S_{A,Q}]$ can be easily estimated from the stationary distribution \vec{x} as follows:

$$E[S_{A,Q}] = \sum_{i=1}^{M_E M_T} \sum_{k=0}^K x_{i,k} k. \quad (34)$$

Finally, substituting (34) and (33) to (31) we get:

$$E[S_{T,Q}] = \sum_{i=1}^{M_E M_T} \sum_{k=0}^K x_{i,k} k - \sum_{i=1}^{M_E} \pi_{E,i} \sum_{j=1}^{M_E} p_{E,ij}. \quad (35)$$

9. Conclusion

In this paper we firstly proposed an extension for existing wireless channel models to the case of mobility-dependent behavior. For this model we provide suitable parametrization methods using either information of measurements of the signal strength or classic large-scale propagation models. Then, we extended the proposed wireless channel model to the small-scale propagation characteristics. To use the model in performance evaluation studies we defined the data-link layer model using the cross-layer mapping.

The proposed data-link layer model can be used in performance evaluation studies of the data-link layer protocols in presence of signal changes caused by movement of the user between areas with qualitatively or quantitatively different propagation characteristics. The proposed cross-layer mapping allows to avoid computationally expensive physical layer simulations when performing performance evaluation studies. We outlined applications of the proposed approach and showed how to obtain performance characteristics of applications using those results available in classic queuing theory.

REFERENCES

1. A. Longley and P. Rice. Prediction of tropospheric radio transmission loss over irregular terrain: as computer method. Technical report: Erl 79-its 67, ESSA, 1968.
2. R. Edwards and J. Durkin. Computer predictions for service area for VHF mobile radio networks. *Proceedings of the IEE*, 116(9):1493–1500, 1969.
3. T. Okumura, E. Omori, and Fakuda K. Field strength and its variability in VHF and UHF land mobile service. *Review of electrical communication laboratory*, 16(9/10):825–873, September/October 1968.
4. M. Feuerstein, K. Blackard, T. Rappaport, S. Seidel, and H. Xia. Path loss, delay spread, and outage models as functions of antenna height for micro-cellular system design. *IEEE Tran. on Veh. Tech.*, 43(3):487–498, August 1994.
5. A. Saleh and R. Valenzuela. A statistical model for indoor multipath propagation. *IEEE JSAC*, 5(2):128–137, February 1987.
6. T. Rappaport. Statistical channel impulse response models for factory and open plan building radio communication system design. *IEEE Trans. on Comm.*, 39(5):794–806, May 1991.
7. D. Durgin and T. Rappaport. Theory of multipath shape factors for small-scale fading wireless channels. *IEEE Trans. on Ant. and Propag.*, 48:682–693, May 2000.
8. M. Krunz and J.-G. Kim. Fluid analysis of delay and packet discard performance for QoS support in wireless networks. *IEEE JSAC*, 19(2):384–395, February 2001.
9. M. Krunz and J.-G. Kim. Delay analysis of selective repeat ARQ for a markovian source over a wireless channel. *IEEE Trans. on Veh. Tech.*, 49(5):1968–1981, September 2000.
10. M. Zorzi, R. Rao, and L. Milstein. ARQ error control for fading mobile radio channels. *IEEE Trans. on Veh. Tech.*, 46(2):445–455, May 1997.
11. M. Zorzi and R. Rao. Perspectives of the impact of error statistics on protocols for wireless networks. *IEEE Pers. Comm.*, 6(5):32–40, October 1999.
12. T. Rappaport. *Wireless communications: principles and practice*. Communications engineering and emerging technologies. Prentice Hall, 2nd edition, 2002.
13. P. Green and R. Sibson. Computing dirichlet tessellations in the plane. *Computer Journal*, 21:168–173, 1978.
14. M. Hata. Empirical formula for propagation loss in land mobile radio services. *IEEE Trans. on Veh. Tech.*, VT-29(3):317–325, August 1980.
15. S. Seidel. Path loss, scattering and multipath delay statistics in four european cities of digital cellular and microcellular radiotelephone. *IEEE Trans. on Veh. Tech.*, 40(4):721–730, November 1991.
16. Q. Zhang and S. Kassam. Finite-state markov model for Rayleigh fading channels. *IEEE Trans. on Comm.*, 47(11):1688–1692, November 1999.
17. J. Swarts and H. Ferreira. On the evaluation and application of markov channel models in wireless communications. In *Proc. VTC'99*, pages 117–121, 1999.